



Synthesis, structural determination, theoretical studies and catalytic activity of Mn(II) complex of *N*-isonicotinyl phosphoric triamide ligand



Maryam Rajabi^a, Khodayar Gholivand^{b,*}, Rasool Salami^b, Foroogh Molaei^b, Jérôme Thibonnet^c, Karim Zare^a, Farzaneh Fadaei Tirani^d, Kurt J. Schenk^d

^a Department of Chemistry, Science and Research Branch, Islamic Azad University, P.O. Box 14515-775, Tehran, Iran

^b Department of Chemistry, Faculty of Sciences, Tarbiat Modares University, P.O. Box 14115-175, Tehran, Iran

^c Université François Rabelais, Département de Chimie, 32 Avenue Monge, 37200 Tours, France

^d CCC-IPSB, École Polytechnique Fédérale de Lausanne, Le Cubotron, Dorigny, CH-1015 Lausanne, Switzerland

ARTICLE INFO

Article history:

Received 10 November 2014

Received in revised form 23 February 2015

Accepted 11 April 2015

Available online 18 April 2015

Keywords:

Mn(II) complex
Phosphoric triamide
Crystal structure
DFT calculations
Epoxidation

ABSTRACT

A new *N*-isonicotinyl phosphoric triamide ligand with the formula 4-NC₅H₄C(O)NHP(O)(NC₄H₈)₂ (**L**) was synthesized and characterized by ¹H, ¹³C, ³¹P NMR and IR spectroscopies. The reaction of MnCl₂·4H₂O with **L** led to the formation of a new 3D system {MnL₂Cl₂}_n·34CH₃OH (**C**₁). X-ray crystallographic data revealed that the ligand binds to the neighboring manganese ions through the nitrogen atom of pyridine (N_{py}) and the oxygen atom of phosphoryl (O_p) in a bidentate manner. The Mn(II) centers showed a distorted *cis*(N_{py}, N_{py}) *cis*(O_p, O_p) *cis*(Cl, Cl) octahedral configuration. In order to compare the relative stability of **C**₁ (with *all-cis* configuration) and its possible *all-trans* isomer, **C**₁, density functional theory (DFT) calculations were performed and the results showed the preference of **C**₁ over **C**₁ from energy point of view. Quantum theory of atoms in molecules (QTAIM) analysis was applied to elucidate the nature of interactions, and the results suggested an ionic character (closed-shell interaction) for Mn–O_p bond, and a partial covalent contribution for Mn–N_{py} interaction. Natural bond orbital (NBO) analysis was also used to calculate the charge distribution on atoms in the complex. The complex **C**₁ showed efficient catalytic activity in the oxidation reaction of some alkenes to their corresponding epoxides. In addition, the effect of temperature and reaction time on the conversion and selectivity of cyclohexene epoxidation reaction in the presence of **C**₁ as catalyst was investigated.

© 2015 Elsevier B.V. All rights reserved.

1. Introduction

The chemistry of pyridinecarboxamides is quite interesting mainly because of their biological and chemotherapeutical properties. Isonicotinamide (4-pyridinecarboxamide) has also pharmaceutical interest for its anti-tubercular, anti-pyretic and anti-bacterial properties, and mixed salts of this molecule has found extensive use in drug industry [1,2]. Besides, some isonicotinamide-based compounds are promising reactivators for the acetylcholinesterase inhibited by sarin [3] and paraoxon organophosphorus agent [4].

Carbacylamidophosphates (CAPH) containing [C(O)NHP(O)] structural framework have been known for a considerable time [5–14]. The main interesting feature of CAPH ligands is the bidentate or μ²-bidentate chelate character of their coordination to the metal [15,16]. Furthermore, complexes of CAPH ligands including

iso(nicotinamide) with an extra donor site (N_{py}) with Sn [17] and Er [18] have been reported.

On the other hand, manganese complexes with diverse ligands are known for their antibacterial [19–21], anticancer [22–24], anti-fungal [25,26], and catalytic activities [27]. We have previously reported the first Mn(II) complex of a CAPH ligand containing isonicotinamide with the formula {Mn[4-NC₅H₄C(O)NHP(O)(NC₆H₁₂)₂Cl₂]}_n. In this complex, the oxygen atom of phosphoryl group (O_p) and the nitrogen atom of pyridine ring (N_{py}) are the two dominant coordination sites towards Mn(II) with *all-trans* configuration for the identical ligands [28]. Here, we present the synthesis, crystal structure, and spectroscopic characterization of bis-[*N*-isonicotinyl, *N'*, *N''*-bis(pyrrolidinyl) phosphoric triamide] Mn(II) dichloride complex (**C**₁) with *all-cis* structure. Since, density functional theory (DFT) is commonly used to examine the structural and electronic characteristics of transition metal complexes, the experimental studies on **C**₁ have been accompanied by DFT calculations and natural bond orbital (NBO) analysis. The stability and structural parameters of **C**₁ (*all-cis*) and its *all-trans* model (**C**₁)

* Corresponding author. Tel.: +98 21 82883443; fax: +98 21 82883455.

E-mail address: gholi_kh@modares.ac.ir (K. Gholivand).

have been also compared. The molecular descriptors derived from the electron density properties and computed at the bond critical points as defined by quantum theory of atoms in molecules (QTAIM) analysis, have been used to gain some insights into the Mn–L interactions. Additionally, the effectiveness of **C**₁ as a catalyst for the epoxidation of some alkenes is demonstrated. To our knowledge, this is the first report on the catalytic activity of Mn–CAPH complex in epoxidation reactions.

2. Experimental

2.1. Materials and methods

All chemicals and solvents were of reagent grade and obtained commercially without further purification. Melting points were obtained with an electrothermal instrument. IR spectra were recorded on a Nicolet 510P spectrophotometer using KBr disk. NMR spectra were recorded on a Bruker Avance DRX-500 spectrometer. ¹H and ¹³C chemical shifts were measured relative to the internal TMS, and ³¹P chemical shift was determined relative to 85% H₃PO₄ as the external standard. The products of oxidation reactions were determined and analyzed by an HP Agilent 6890 gas chromatograph equipped with a HP-5 capillary column (phenyl methyl siloxane 30 m 320 lm 0.25 lm), and a flame ionization detector.

2.2. Synthesis of *N*-isonicotinyl, *N*', *N*'-bis(pyrrolidinyl) phosphoric triamide, 4-NC₅H₄C(O)NHP(O)(NC₄H₈)₂ (**L**)

N-isonicotinyl phosphoramidic dichloride, 4-NC₅H₄C(O)NHP(O)Cl₂, was prepared and purified according to the literature [17]. A solution of pyrrolidine 8 mmol (0.66 mL) in dry acetonitrile (20 mL) was added dropwise to a solution of 4-NC₅H₄C(O)NHP(O)Cl₂ 2 mmol (0.48 g) in dry acetonitrile (20 mL) at 0 °C. After 4 h stirring, the solvent was evaporated and the brown transparent oily residue was washed with acetone to remove the pyrrolidine salt and the filtrate was powdered by *n*-heptane.

Yield: 70%. m.p. 164 °C. ¹H NMR (500.13 MHz, DMSO-*d*₆): δ = 1.72–1.82 (m, 8H_{aliphatic}), 3.09–3.20 (m, 8H_{aliphatic}), 7.78 (dd, ⁵J_{PH} = 1.6 Hz, ³J_{HH} = 4.5 Hz, 2H_{pyridine}), 8.72 (dd, ⁶J_{PH} = 1.5 Hz, ³J_{HH} = 4.5 Hz, 2H_{pyridine}), 9.49 (d, ²J_{PNH} = 6.5 Hz, 1H, NH_{amide}) ppm. ¹³C NMR (125.76 MHz, DMSO-*d*₆): δ = 25.8 (d, ³J_{PC} = 8.5 Hz), 45.9 (d, ²J_{PC} = 4.9 Hz), 121.8 (s), 141.0 (d, ³J_{PC} = 8.7 Hz, C_{ipso}), 150.1 (s), 166.9 (s, C=O) ppm. ³¹P NMR (202.46 MHz, DMSO-*d*₆): δ = 6.47 (m) ppm. IR (KBr, cm⁻¹): 3075 (mw), 2930 (ms), 1678 (s, C=O), 1553 (w), 1494 (mw), 1443 (vs), 1268 (ms), 1215 (s), 1179 (s, P=O), 1111 (m), 1083 (s), 1014 (m), 873 (m), 821 (ms), 748 (m), 699 (mw), 580 (mw), 538 (mw), 467 (mw).

2.3. Synthesis of bis-[*N*-isonicotinyl, *N*', *N*'-bis(pyrrolidinyl) phosphoric triamide] Mn(II) dichloride, {Mn[4-NC₅H₄C(O)NHP(O)(NC₄H₈)₂Cl₂]_n·34CH₃OH (**C**₁)

MnCl₂·4H₂O 0.5 mmol (0.10 g) was added to a solution of **L** 1 mmol (0.31 g) in methanol (15 mL) and stirred for 4 h. Upon slow evaporation of the filtrate at room temperature, suitable colorless prism crystals of the complex **C**₁ were isolated. **C**₁ is soluble in ethanol, methanol and acetonitrile.

Yield: 50%. m.p. 191–192 °C. IR (KBr, cm⁻¹): 3446 (br), 3096 (br), 2965 (m), 2874 (m), 1686 (s, C=O), 1617 (w), 1558 (w), 1451 (vs), 1268 (m), 1217 (m), 1166 (m, P=O), 1015 (mw), 917 (w), 820 (mw), 795 (w), 685 (w), 582 (w), 544 (mw), 477 (w).

2.4. Crystal structure determination

Suitable single crystals of **C**₁ were mounted on a glass fibre. Data collections were carried out at room temperature on a Bruker-Nonius Kappa-CCD-diffractometer equipped with graphite-monochromatized Mo Kα radiation (λ = 0.71073 Å). Cell parameters were retrieved and refined using the DENZO-SMN [29] software on all reflections. Data reduction was performed with the DENZO-SMN software. The structure was solved by SIR2004 [30] and refined with the program SHELXL-2014/7 [31]. After obtaining the anisotropic refinement of the structural model, the remaining residua suggested very disordered methanol molecules. So, by computing the mass and number of electrons in the obvious void by means of the SQUEEZE-option of the PLATON-program [32], it was found that the complex is solvated with six methanol molecules per formula unit (a reasonable simplification in view of the possible loss of solvent). According to the SQUEEZE-results, thirty-four molecules of methanol were included in the final refinement as a fixed contribution.

All non-hydrogen atoms were refined anisotropically. Three of the pyrrolidine rings were split into two orientations. The major and minor parts were refined anisotropically, but distance and similarity restraints (SADI, SIMU and SAME) had to be applied for a convergent least-square refinement yielding site occupancy ratios of 0.39(3)/0.61(6), 0.20(3)/0.80(6) and 0.46(7)/0.54(2). Hydrogen atoms were placed in geometrically idealized positions, and constrained to ride on their parent atoms. Crystal data and experimental details of the structure determination for **C**₁ are listed in Table 1.

2.5. Computational details

The calculations were carried out using the GAUSSIAN 03 package [33]. Density functional calculation using the Becke's three parameter hybrid functional combined with the Lee–Yang–Parr correlation function (B3LYP) [34] was chosen among the DFT methods due to its good performance in molecular structure and force field determinations [35]. For **C**₁, a fragment related to the *all-cis*

Table 1
Crystallographic data for **C**₁.

Compound	C ₁
Empirical formula	C ₂₈ H ₄₂ Cl ₂ N ₈ O ₄ P ₂ Mn·6(CH ₃ O)
Formula weight	934.78
<i>T</i> (K)	293(2)
Crystal system, space group	trigonal, <i>P</i> 3 ₁ 2 1
<i>a</i> (Å)	16.7451(5)
<i>b</i> (Å)	16.7451(5)
<i>c</i> (Å)	25.7864(9)
α (°)	90
β (°)	90
γ (°)	120
<i>V</i> (Å ³)	6261.8(4)
<i>Z</i>	6
<i>D</i> _{calc} (Mg m ⁻³)	1.470
Absorption coefficient (mm ⁻¹)	0.584
<i>F</i> (000)	2933
Crystal size (mm)	0.2 × 0.16 × 0.04
θ range for data collection (°)	1.61–27.71
Reflections collected	9668
Independent reflections	5340 [<i>R</i> _{int} = 0.0450]
Completeness to θ (%)	0.99/0.55
Data/restraints/parameters	5340/498/548
Flack parameter	0.002(14)
Goodness-of-fit (GOF) on <i>F</i> ²	1.026
Final <i>R</i> indices	<i>R</i> ₁ = 0.0726, <i>wR</i> ₂ = 0.2018
<i>R</i> indices (all data)	<i>R</i> ₁ = 0.1293, <i>wR</i> ₂ = 0.2523
Largest difference in peak and hole (e Å ⁻³)	0.522 and –1.025

configuration was extracted from the X-ray atomic coordinates, and was fully optimized in the gas phase along with its *all-trans* isomer (C_1) and the ligand. 6-311G* standard basis set in optimization was used in this study for **L**, C_1 and C_1 . Natural Bond Orbital (NBO) analysis [36] was performed at B3LYP/6-31+G* level. QTAIM analysis was performed with the help of AIM 2000 software [37] using the wave functions generated at B3LYP/6-311+G* level.

2.6. Catalytic experiments

To a mixture of alkene (1.0 mmol), chlorobenzene (0.5 mmol) as an internal standard, C_1 0.1 mol%, and acetic acid (0.5 mmol) in acetonitrile (2 mL) under Ar atmosphere at 0 °C was slowly added 1 equiv. of 30% H₂O₂ in acetonitrile (within a period of 20 min). The reaction mixture was stirred in an ice bath for 2 h, and then extracted with Et₂O. The reaction products were immediately analyzed by GC.

3. Results and discussion

3.1. Synthesis of **L** and C_1

Ligand **L** was simply prepared by the reaction of 1 equiv. of *N*-isonicotinyl phosphoramidic dichloride intermediate with 4 equiv. of pyrrolidine in acetonitrile solution. The pyrrolidiny hydrochloride salt formed during the reaction was filtered by washing with acetone. The reaction between **L** and MnCl₂·4H₂O with the ligand:metal composition of 2:1 in methanol afforded six-coordinated Mn(II) complex with polymeric structure (C_1). The synthesis pathway is illustrated in Scheme 1.

3.2. Spectroscopic characterization

Among the spectroscopic techniques employed to infer the binding mode of isonicotinamide [2,38], IR spectroscopy is the most widely used method. The vibrational modes associated with amidic group and pyridine ring give important information about the coordination fashion of phosphoramidate ligands including isonicotinamide moiety. By coordination of the pyridine type nitrogen to metal ion, some vibrational modes shift to higher frequencies for

coupling with M–N_{py} bond vibrations [39]. Additionally, it is well established that, if coordination takes place through carboxyl oxygen, a shift to lower frequency of the ν_{C=O} is expected when compared to that of the free ligand [40]. When a carbacylamidophosphate coordinates to metal ion *via* its P=O site, the value of its ν_{P=O} becomes smaller while the amount of ν_{C=O} gets greater [17,41].

Comparing the IR spectrum of the **L** ligand with that of the C_1 complex, we observed that stretching vibrations of pyridine ring and carbonyl of the ligand (1580 and 1678 cm⁻¹, respectively) shifted to higher frequencies in the complex (1617 and 1686 cm⁻¹, respectively), showing the involvement of N_{py}, and non-involvement of carbonyl in the coordination. A negative shift in ν_{P=O} indicates binding through the phosphoryl oxygen atom to Mn(II) (1179 cm⁻¹ in **L** and 1166 cm⁻¹ in C_1). A higher frequency shift of the N–H stretching vibration due to the formation of the complex (3420 cm⁻¹ in **L** and 3446 cm⁻¹ in C_1) is in agreement with the presence of weaker hydrogen bonds in the complex in comparison with the ligand [42]. The weak bands at 544 and 477 cm⁻¹ may be attributed to Mn–O_p and Mn–N_{py} vibrations, respectively.

¹H NMR spectrum of **L** showed the value of 6.5 Hz for ²J_{(PNH)amide}, and also the long-range ⁿJ_{P,H} (n = 5, 6) coupling constants in the range of 1.5–1.6 Hz. Such interesting long-range couplings have been observed only in few compounds till now [43]. It should be noted that due to the paramagnetic nature of C_1 , the NMR spectra and solution structure of the complex could not be studied.

3.3. Crystal structure

Complex C_1 crystallizes in the trigonal space group *P* 3₁ 2 1 and Z = 6 in the unit cell. The molecular structure of C_1 with the atom-labelling scheme is depicted in Fig. 1, and selected bond lengths and angles are summarized in Table 2.

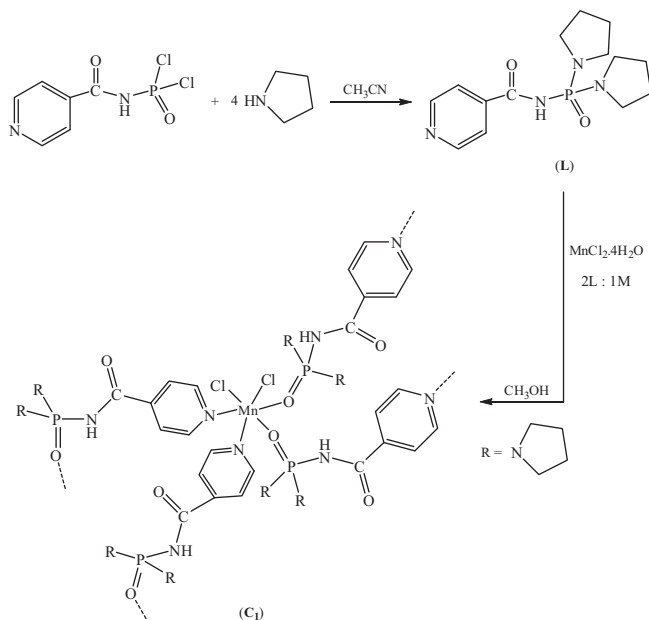
The Mn(II) ion is six-coordinated by two N_{py} and two O_p atoms from the bridged bidentate ligand, and two chlorine atoms, forming an octahedral geometry around the central metal ion (Fig. 1). Two *N*-coordinated and two *O*-coordinated ligands as well as two chlorines in *cis* positions form an *all-cis* configuration.

The *cisoid* angles around Mn(II) ion are 83.7(2)–98.17(9)°, and the *transoid* O_p–Mn–N_{py}, N_{py}–Mn–Cl, and O_p–Mn–Cl angles deviate slightly from 180° to the range of 169.18(14)–175.6(2)°, indicating a slight distortion of the octahedral geometry. The Mn–N_{py} bond lengths are 2.293(6) and 2.337(7) Å, in the range of the distances in Mn(II) complexes with typical nitrogen donor ligands containing pyridine rings [44]. One of the Mn–N_{py} bonds is longer than that for {Mn[4-NC₅H₄C(O)NHP(O)(NC₆H₁₂)₂Cl₂]_n (2.308(3) Å) [28]. The Mn–O_p distances, 2.178(5) and 2.212(5) Å, are larger than those in Mn(Cl₃CC(O)NP(O)(NHC₃H₅)₂)₂(C₁₀H₈N₂) (2.115(2) and 2.147(2) Å) [45], and in the range of the reported values for Mn(II) complexes with dichalcogenoimidodiphosphonate ligands [46]. One of the Mn–O_p bond distances is longer than the value reported for Mn–O_p (2.1713(1) Å) in {Mn[4-NC₅H₄C(O)NHP(O)(NC₆H₁₂)₂Cl₂]_n [28].

Phosphoryl and carbonyl groups are *anti* to each other as a result of dipole–dipole repulsion with the values of 165.4(7)° and –179.0(7)° for O–P–N–C_{carbonyl} torsion angles.

Complex C_1 produces hydrogen bonds including intramolecular C(18)–H(18)...O(4), C(24)–H(24B)...O(4) and N(1)–H(1)...Cl(1), and intermolecular N(6)–H(6)...Cl(2) and C(16)–H(16)...Cl(2). Hydrogen bonds data are given in Table 3.

We have previously shown that upon coordination of phosphorylated isonicotinamide and nicotinamide compounds to Sn [17,47], binding occurs through either O_p or N_{py}, or both of the donor sites participate in coordination. The coordination pattern



Scheme 1. Preparation pathway of **L** and C_1 .

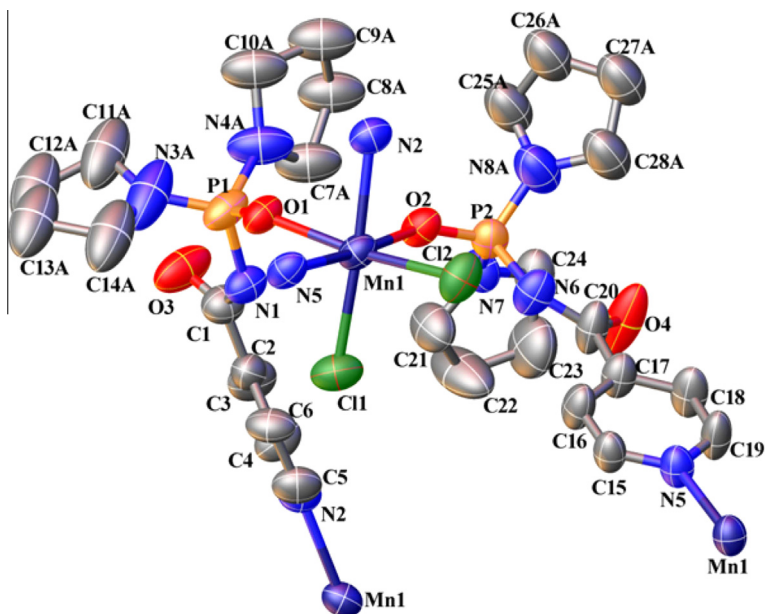


Fig. 1. The molecular structure of **C₁** with its atom (50% probability level) labelling scheme. Hydrogen atoms were omitted for clarity. Note that only the major of the two orientations of the disordered pyrrolidine rings is shown.

Table 2

Selected geometrical parameters for **C₁** (solid state and gas phase) and **C₁** (gas phase) calculated at B3LYP/6-311G*.

Compound	C₁	C₁	C₁
<i>Bond lengths (Å)</i>	X-ray	Calc.	Calc.
Mn(1)–O(1)	2.212(5)	2.076	2.152
Mn(1)–O(2)	2.178(5)	2.081	2.143
Mn(1)–N(2) ⁱ	2.337(7)	2.002	2.029
Mn(1)–N(5)	2.293(6)	2.025	2.051
Mn(1)–Cl(1)	2.502(2)	2.383	2.439
Mn(1)–Cl(2)	2.530(2)	2.463	2.451
P(1)–O(1)	1.463(5)	1.519	1.489
P(2)–O(2)	1.481(6)	1.511	1.497
P(1)–N(1)	1.697(8)	1.715	1.726
P(1)–N(3B)	1.611(15)	1.655	1.655
P(1)–N(4B)	1.563(16)	1.650	1.651
<i>Bond angles (°)</i>			
N(2) ⁱ –Mn(1)–O(2)	86.7(2)	87.889	97.159
N(5)–Mn(1)–O(2)	175.6(2)	177.289	90.164
N(2) ⁱ –Mn(1)–Cl(1)	174.26(18)	177.844	91.409
N(2) ⁱ –Mn(1)–Cl(2)	87.32(18)	90.735	87.861
O(1)–Mn(1)–Cl(1)	91.03(18)	88.505	87.225
O(1)–Mn(1)–Cl(2)	169.18(14)	178.714	88.617

Symmetry code (i): 1 – x, –x + y, 1/3 – z.

Table 3

Hydrogen bond data for **C₁** (distances in Å and angles in °).

D–H...A	d(D–H)	d(H...A)	d(D...A)	∠DHA
N(1)–H(1)...Cl(1)	0.86	2.52	3.339(9)	160
C(9B)–H(9BA)...Cl(1)	0.97	2.79	3.60(2)	142
N(6)–H(6)...Cl(2)	0.86	2.33	3.160(8)	163
[2 – x, 1 – x + y, 1/3 – z]				
C(16)–H(16)...Cl(2)	0.93	2.83	3.509(12)	131
[2 – x, 1 – x + y, 1/3 – z]				
C(11B)–H(11C)...O(3)	0.97	2.52	3.24(3)	130
C(18)–H(18)...O(4)	0.93	2.38	3.273(14)	160
C(24)–H(24B)...O(4)	0.97	2.34	2.975(16)	122
C(10B)–H(10D)...N(3B)	0.98	2.49	2.89(3)	104

via both O_p and N_{py} has also been observed in the complexation of these ligands with Er [18] and Mn [28], producing 1D chains and a 3D network, respectively. On the other hand, although for carbonylamidophosphates (and their deprotonated form) binding through both phosphoryl and carbonyl groups have been reported [6,16,42,45], coordination from P=O in C(O)NHP(O) fragment is more probable than C=O, due to higher polarizability of phosphoryl group [48]. Monodentate fashion of such ligands have been observed in coordination with Ln(III), Sb, Sn(IV) and U [49].

Here each Mn(II) atom is linked to four neighboring metal ions through the bridging μ-O,N-phosphoric triamide ligands (**L**) to produce an octahedral 3D framework (Fig. 2). Complex **C₁** can be simplified as a four-connected uninodal net. This net topology is qtz with (6⁴.8²) point symbol and vertex symbol (6.6.6².6².8⁹.8⁹). The simplified 3D network of **C₁**, with qtz topology, is shown in Fig. 3.

3.4. DFT calculations

As stated in the previous section, the ligands adopt *all-cis* configuration around the Mn(II) ions in complex **C₁**. Another possible structure is *all-trans* in which the same donor atoms are located in *trans* positions (**C₁**). In this regard, we used DFT calculations to compare the relative stability and structural parameters of **C₁** with its *all-trans* analogue (**C₁**) in the gas phase. The optimized structures are shown in Fig. 4, and the optimized values for selected geometrical parameters are presented in Table 2. The calculated Mn–O_p, Mn–N_{py} and Mn–Cl bond distances of **C₁** are shorter in comparison with the X-ray results, probably owing to neglecting the effect of the neighboring units interactions in the gas phase. The rest of the structural parameters show good agreement with the experimental values in **C₁**. Comparison of the calculated Mn–O_p and Mn–N_{py} bond lengths in **C₁** and **C₁** (Table 2) shows shorter distances in **C₁**, specifically in case of Mn–O_p bonds. The potential energy difference between the two isomers (**C₁** and **C₁**) is 31.61 kcal/mol, indicating the preference of *all-cis* isomer (**C₁**) in the gas phase comparing to the *all-trans* one (**C₁**). The higher stability of the *cis* isomer in the gas phase has also been

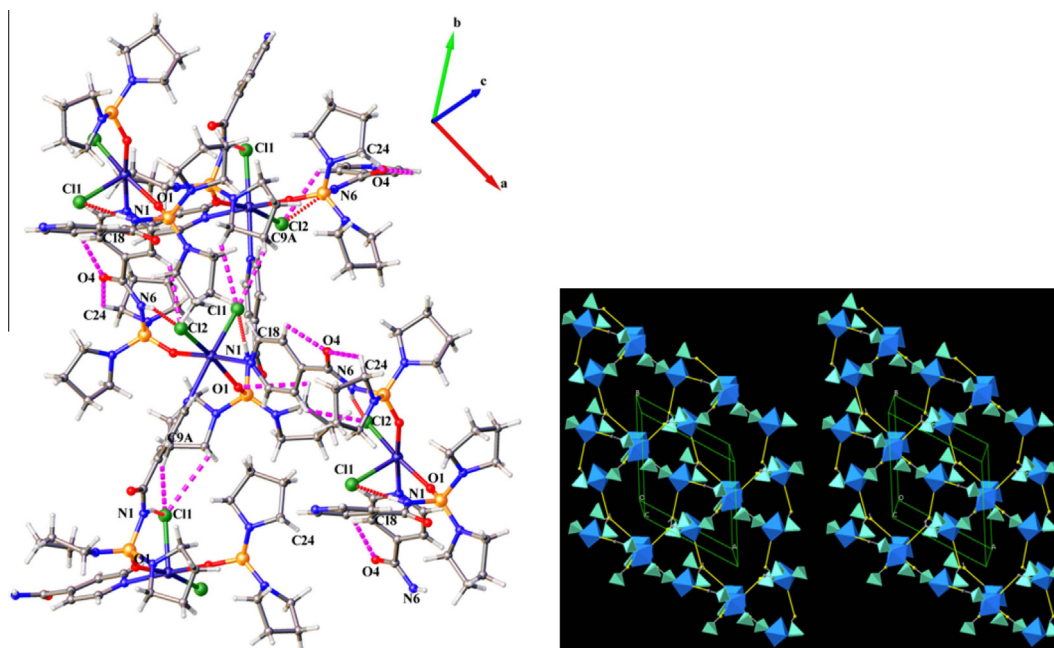


Fig. 2. 3D representation of C_1 formed by intra- and intermolecular interactions (on the left) and a stereoscopic view of the crystal packing along the c axis (on the right).

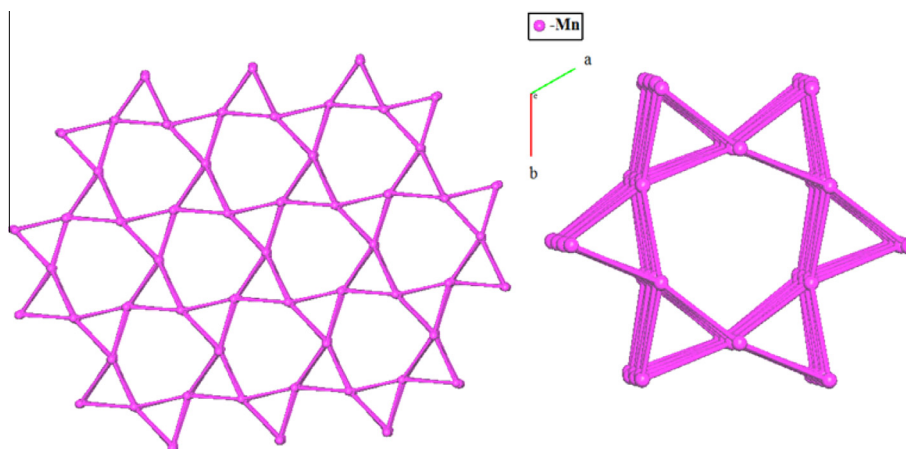


Fig. 3. The simplified 3D network of C_1 , with qtz topology, in which the Mn and L ligands are shown as pink balls and links, respectively. (For interpretation of the references to colour in this figure legend, the reader is referred to the web version of this article.)

reported for $\text{SnCl}_4 \cdot 2\text{L}$ adducts, where L is a phosphoryl donor ligand [50].

3.5. QTAIM analysis

According to the QTAIM theory, the electron density (ρ), its Laplacian ($\nabla^2\rho$) and electronic energy density (H_r) at a bond critical point (bcp) provide information about the characteristics of the bond [51]. In general, ρ is greater than 0.20 au in a shared (covalent) bonding and less than 0.10 au in a closed-shell interaction (e.g., ionic, van der Waals and hydrogen bonding). Laplacian is essentially a second derivative, and its sign indicates the regions of local electronic charge concentration ($\nabla^2\rho < 0$) or depletion ($\nabla^2\rho > 0$) with respect to the immediate neighborhood. The electronic energy density (H_r) at a bond critical point, instead of $\nabla^2\rho$, is a more appropriate index to better characterize a weak interaction. The H_r sign determines whether the accumulation of charge at a given critical point is stabilizing ($H_r < 0$) or destabilizing ($H_r > 0$) [52].

The values of ρ , $\nabla^2\rho$ and H_r computed at the critical points of Mn– N_{py} and Mn– O_{p} bonds are listed in Table 4. Here, the strongly polarized character of Mn–L interaction is evident from the values of the charge density at the critical points of Mn–L bonds. The small estimated ρ values at the Mn– N_{py} bond paths (0.081 and 0.085 au) and the values of $\nabla^2\rho > 0$ and $H_r < 0$ suggest that the interaction is principally electrostatic in nature with a partial covalent contribution. In case of Mn– O_{p} , the small values of electronic density (0.053 and 0.055 au) and the positive values of $\nabla^2\rho$ and H_r , reveal the essential ionic nature of the interaction. The same trend has been found for Mn–L interaction in C_1 , and another important point is that both the Mn– N_{py} and Mn– O_{p} charge densities of C_1 are slightly less than those of C_1 , corresponding to the relatively stronger interactions in C_1 .

As seen in Table 4, a decrease in charge density at P=O bond in both C_1 and C_1 (0.213–0.220 au) with respect to that of the free ligand L (0.230 au) is in accordance with the lengthening of phosphoryl group upon complexation (calculated P=O values: 1.489–1.512 Å in C_1 and C_1 , and 1.487 Å in L). Furthermore, less negative H_r values in the C_1 and C_1 complexes in comparison to the ligand

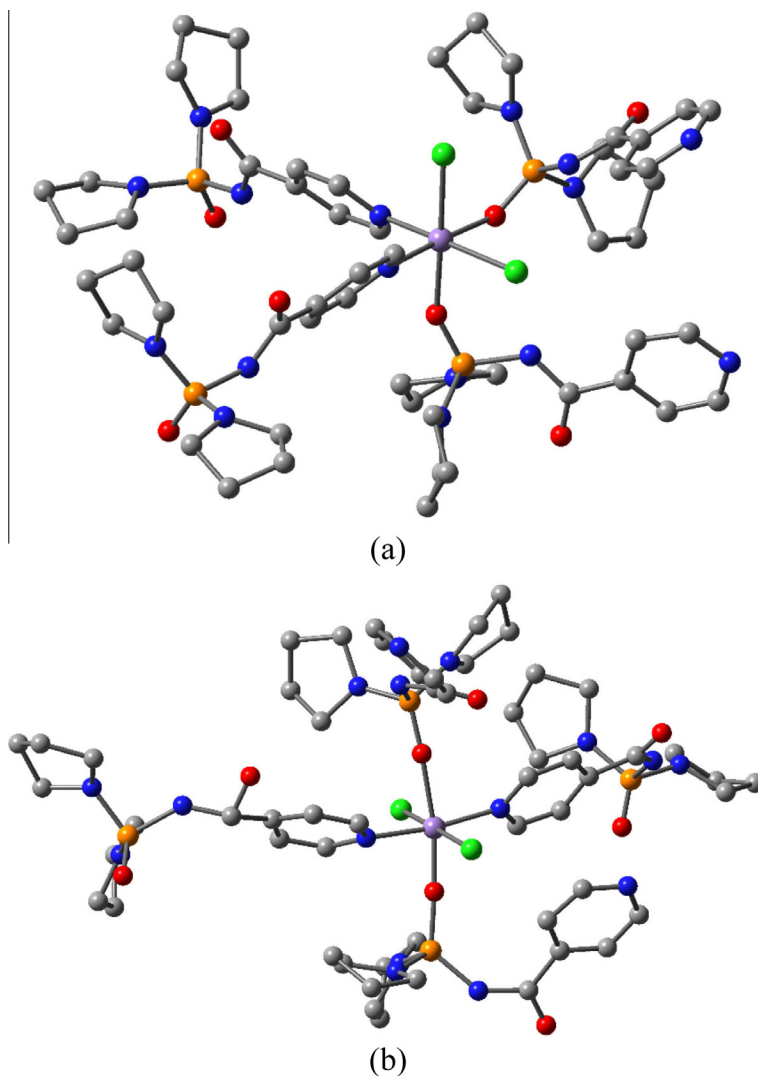


Fig. 4. Optimized structure of (a) C_1 (all-cis) and (b) C_1 (all-trans) isomers.

Table 4

Calculated QTAIM parameters (electron density, ρ , Laplacian, $\nabla^2\rho$, and total electronic energy density, H_r) at selected critical points.

Compounds	Mn–N _{py}			Mn–O _p			P=O		
	ρ	$\nabla^2\rho$	H_r	ρ	$\nabla^2\rho$	H_r	ρ	$\nabla^2\rho$	H_r
L	–	–	–	–	–	–	0.230	1.399	–0.173
C₁	0.081	0.419	–0.010	0.055	0.389	0.005	0.213	1.191	–0.156
	0.085	0.457	–0.012	0.053	0.372	0.005	0.216	1.248	–0.157
C'₁	0.074	0.412	–0.008	0.041	0.289	0.006	0.219	1.351	–0.156
	0.079	0.462	–0.009	0.042	0.280	0.005	0.220	1.307	–0.160

indicate a decrease in the covalent contribution of the P=O bond by coordination and electron donation to the metal ion.

3.6. NBO analysis

Natural bond orbital (NBO) analysis gives the natural electron population and the natural charge for each atom. The interaction between filled (donor) NBOs and empty (acceptor) NBOs leads to the loss of occupancy from the localized NBOs of the idealized Lewis structure into the empty non-Lewis orbitals. The stabilization energy, ΔE_{ij} , associated with such delocalization is given by the second-order perturbative correction [53]. For C_1 , the electronic configuration of Mn is: [core] $4s^{0.22} 3d^{5.76} 4p^{0.57} 4d^{0.03}$,

17.992 core electrons, 6.558 valence, and 0.0201 Rydberg electrons giving 24.588 total electrons. The calculated natural charge on Mn(II) ion is +0.412 (difference between 24.588 and the total number of electrons in the isolated Mn atom (25)). The distribution of 5.76 electrons among the 3d orbitals is as follows: d_{xy} 1.01778; d_{xz} 1.78900; d_{yz} 1.20813; d_{xy}^2 1.19085 and d_z^2 0.55852. The high 3d-electron population of 5.76 is accounted to $L \rightarrow d_{Mn}$ charge transfer. Also the natural electron configuration for Mn(II) can be representative of the LMCT, in which the metal 4s, 4p and 4d orbitals are partially occupied. The natural charge on the metal ion indicates that the charge donations from the ligand to the central ion have advantage over the back donations from the metal to the ligand. The stabilization energies calculated in the NBO analysis ($E^{(2)}$)

showed that the lone pairs localized on the donor atoms of phosphoramidate ligand donate the charge to Mn(II). The $E^{(2)}$ value for the $LP(N_{py}) \rightarrow LP^*(Mn)$ and $LP(O_p) \rightarrow LP^*(Mn)$ electronic delocalizations is 17.53 and 13.78 kcal/mol, respectively. The electronic configurations and the natural charges on the atoms calculated by NBO analysis are gathered in Table 5. It is seen that the negative natural charges on N_{py} and O_p atoms decrease on complexation, where these atoms transfer electron to Mn(II) ion, and more reduction is observed for nitrogen in accordance with its greater $E^{(2)}$ value. Besides, upon coordination of O_p to the metal center, the positive charge on the P atom becomes higher in the complex than in the free ligand, due to the electronic charge transfer to the donor oxygen atom and also the polarization effect. The hybridization of the lone pair of the phosphoryl oxygen, $LP(O_p)$, and the nitrogen atom of pyridine ring, $LP(N_{py})$, take more p character in the complex C_1 ($sp^{1.97}$, $sp^{2.80}$ and $sp^{2.83}$, $sp^{2.80}$, respectively) as compared to its free ligand ($sp^{0.53}$ and $sp^{2.46}$).

In agreement with the QTAIM analysis results, the values of Wiberg bond indices for Mn– N_{py} bonds (0.1209 and 0.1222) are indicative of a slight covalent character of the interaction, while the values of 0.0889 and 0.0844 for Mn– O_p bonds confirm a predominant ionic character of the interaction.

3.7. Catalytic activity

Olefin epoxidation constitutes a very important reaction in organic synthesis because epoxides are valuable building blocks for a number of subsequent transformations [54]. Manganese is catalytically active in a variety of metalloenzymes [55], and less damaging to the environment compared with many other transition metals. Various manganese complexes ligated with salens, porphyrins and aromatic N -donor ligands are known to be efficient catalysts for the epoxidation of a wide range of alkenes [56]. Herein, we report a simple and efficient catalytic system, which uses complex C_1 as catalyst, acetic acid (CH_3CO_2H) as co-catalyst, and oxidant H_2O_2 for epoxidation of some alkenes.

Epoxidation of olefins was carried out using hydrogen peroxide as oxidant in acetonitrile solvent, and in the presence of C_1 as catalyst. In a search for suitable reaction conditions, the epoxidation of cyclohexene was used as a standard reaction. As shown in Table 6, the obtained yield without co-catalyst is only 11% in 2 h. Among imidazole, ammonium acetate and acetic acid, which were evaluated as co-catalysts, we found acetic acid to be the most effective compound for cyclohexene epoxidation with H_2O_2 . Recently, Costas and co-workers reported that the amount of acetic acid is quite dependent on the nature of manganese complexes [57]. They optimized the amount of acetic acid from 0.35 to 14 equiv. for different manganese complexes. Different molar ratios of co-catalyst to oxidant were investigated while the amount of cyclohexene (1 mmol) was kept constant. The best yield was obtained when the ratio of co-catalyst to oxidant was 0.5 mmol/1 mmol. Table 7 illustrates the effect of temperature and reaction time on the conversion and selectivity of cyclohexene epoxidation. Epoxidation of cyclohexene was carried out by changing the temperature at -30 , 0 and 30 °C. When the temperature was raised

Table 6
Epoxidation of cyclohexene catalyzed by C_1 .^a

Entry	Co-catalyst	Oxidant	Epoxide ^b (%)
1	CH_3COOH (1 mmol)	H_2O_2 (1 mmol)	4 ^c
2	CH_3COOH (1 mmol)	None	None
3	None	H_2O_2 (1 mmol)	11
4	CH_3COOH (1 mmol)	H_2O_2 (1 mmol)	69
5	Imidazole (1 mmol)	H_2O_2 (1 mmol)	26
6	CH_3COONH_4 (1 mmol)	H_2O_2 (1 mmol)	56
7	CH_3COOH (1 mmol)	H_2O_2 (2 mmol)	62
8	CH_3COOH (2 mmol)	H_2O_2 (1 mmol)	65
9	CH_3COOH (1 mmol)	H_2O_2 (0.5 mmol)	48
10	CH_3COOH (0.5 mmol)	H_2O_2 (1 mmol)	70
11	CH_3COOH (0.4 mmol)	H_2O_2 (1 mmol)	64

^a Conditions: Cyclohexene (1 mmol), C_1 catalyst (0.1 mol%) in 2 mL CH_3CN at 0 °C within 2 h.

^b Determined by GC analysis using chlorobenzene as internal standard based on the starting substrate.

^c Non-catalyst.

Table 7
Cyclohexene oxidation in varying reaction temperature and time.^a

Entry	Temperature	Time (h)	Conv. (Yield ^b)%
1	-30 °C	1	33 (30)
2		2	45 (41)
3		3	55 (49)
4		4	58 (50)
5	0 °C	1	55 (55)
6		2	70 (70)
7		3	75 (71)
8		4	77 (68)
9	30 °C	1	25 (18)
10		4	33 (21)

^a Conditions: Cyclohexene (1 mmol), H_2O_2 (1 mmol), CH_3COOH (0.5 mmol) and C_1 (0.1 mol%) in 2 mL CH_3CN at 0 °C within 2 h.

^b Yields based on the epoxides formed.

from -30 °C to 0 °C, the conversion and yield of the reaction were increased. However, by raising the temperature from 0 °C to 30 °C, the conversion and yield of the reaction were reduced, possibly due to more tendency of Mn(II) complex to catalyze H_2O_2 disproportionation at 30 °C. At 0 °C when the time was prolonged to 4 h, the conversion was slightly increased, and no obvious enhancement in the yield of epoxidation was detected. Based on these observations, optimized temperature and time for better yield of cyclohexene to cyclohexene epoxide are obtained at 0 °C within 2 h.

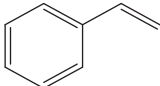
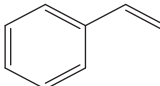
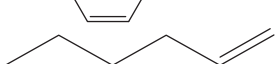
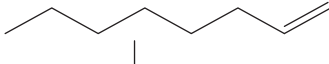
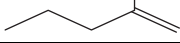
Table 8 presents the results of catalytic experiments on various olefins at optimized conditions (0 °C, 2 h). These data show that the $C_1/CH_3COOH/H_2O_2$ system leads to the epoxidation of aromatic and aliphatic olefin substrates with moderate to high yields. For example, the yields for cyclohexene, cyclooctene, styrene, *cis*- β -methylstyrene, *cis*-stilbene, 1-hexene, 1-octene, and 2-methyl-1-pentene epoxidation are 70%, 78%, 61%, 69%, 28%, 56%, 55%, and 60%, respectively (Table 8). In all cases, the formed epoxides are the main products. It is significant that the epoxidation of *cis*- β -methylstyrene produces only *cis* epoxide, and is completely

Table 5
Atomic charges, hybridizations and electronic configurations at B3LYP/6-31+G* level.

Compounds	Atomic charge			NEC ^a			Hybridization	
	$q(P)$	$q(O_p)$	$q(N_{py})$	O_p	N_{py}		$LP(O_p)$	$LP(N_{py})$
L	2.372	-1.073	-0.441	[core] $2s^{1.81} 2p^{5.26}$	[core] $2s^{1.38} 2p^{4.04} 3p^{0.01} 3d^{0.01} 4p^{0.01}$		$sp^{0.53}$	$sp^{2.46}$
C₁	2.539	-1.052	-0.401	[core] $2s^{1.73} 2p^{5.31} 3p^{0.01}$	[core] $2s^{1.30} 2p^{4.07} 3p^{0.01}$		$sp^{1.97}$	$sp^{2.83}$
	2.529	-1.062	-0.399	[core] $2s^{1.72} 2p^{5.32} 3p^{0.01}$	[core] $2s^{1.30} 2p^{4.07} 3d^{0.02}$		$sp^{2.80}$	$sp^{2.80}$

^a Natural electron configuration.

Table 8
Epoxidation of different substrates by C_1 .^a

Entry	Substrate	Conv. /Yield ^b %
1		70/70
2		78/78
3		67/61
4		75/69 c/t ^c : 99
5		47/28
6		59/56
7		58/55
8		64/60

^a Conditions: The molar ratios for C_1 :substrate: H_2O_2 : CH_3COOH are 1:1000:1000:500 dissolved in 2 mL CH_3CN at 0 °C within 2 h.

^b Determined by GC analysis using chlorobenzene as internal standard based on the epoxides formed.

^c The percent of *cis* isomer obtained.

stereospecific (Table 8, entry 4). This phenomenon may decline the possibility of radical mechanism. The yield of epoxidation for *cis*- β -methylstyrene is better than for styrene (Table 8, entry 3); this shows that the activity of olefins depends on the electron density of the double bond. It is matched with an electrophilic transfer of the oxygen atom from the oxomanganese intermediate to the double bond [58]. Moreover, for aliphatic terminal alkenes, which tend to be the least reactive olefins in epoxidation [56], good yields were obtained under these conditions (Table 8, entries 6–8). The activity of terminal aliphatic olefins is almost independent from steric hindrance and chain length.

The most important characteristics of our catalytic system could be summarized as having low side products with the use of small amount of co-catalyst, and high efficacy for different kinds of olefin substrates.

4. Conclusion

The reaction between the synthesized ligand and $MnCl_2 \cdot 4H_2O$ led to the formation of a new 3D system $\{Mn[4-NC_5H_4C(O)NHP(O)(NC_4H_8)_2]_2Cl_2\}_n \cdot 34CH_3OH$ (C_1). The X-ray diffraction analysis revealed a distorted octahedral geometry around the Mn(II) ions with the *N*-isonicotinyl phosphoric triamide ligand bonded to the metal through N_{py} and O_p atoms. DFT calculations indicated that C_1 with *all-cis* configuration for similar donor atoms was more stable than its related *all-trans* isomer (C_1) in the gas phase. In order to investigate the electronic aspects and the nature of Mn–L interaction, NBO and QTAIM analyses were performed. Based on QTAIM analysis, Mn– N_{py} interaction was found to be mainly electrostatic in nature with partial amount of covalent contribution, and for Mn– O_p , a closed-shell interaction was established. NBO analysis showed strong donor–acceptor interaction

between the donor atoms of ligand and the metal center. In addition, our findings demonstrated the effectiveness of C_1 as a catalyst for oxidation of some alkenes to their corresponding epoxides, which showed moderate to high yields.

Acknowledgements

We are grateful to Tarbiat Modares University and Islamic Azad University, Science and Research Branch (Tehran, Iran) for their support of this research. We also would like to thank Michel Giorgi of Aix-Marseille University for the X-ray experiment.

Appendix A. Supplementary material

CCDC 998974 contains the supplementary crystallographic data for C_1 . These data can be obtained free of charge from The Cambridge Crystallographic Data Centre via www.ccdc.cam.ac.uk/data_request/cif. Supplementary data associated with this article can be found, in the online version, at <http://dx.doi.org/10.1016/j.ica.2015.04.005>.

References

- [1] R.K. Murray, D.K. Granner, P.A. Mayes, V.W. Rodwell, Harper's Biochemistry, 22nd ed., Prentice Hall International Inc, London, 1990.
- [2] S. Yurdakul, A. Ataç, E. Sahin, S. Ide, Vib. Spectrosc. 31 (2003) 41.
- [3] K. Kuca, J. Bielavsky, J. Cabal, M. Bielavska, Tetrahedron Lett. 44 (2003) 3123.
- [4] H.C. Jeong, N.J. Park, C.H. Chae, K. Musilek, J. Kassa, K. Kuca, Y.S. Jung, Bioorg. Med. Chem. 17 (2009) 6213.
- [5] O.N. Rebrova, V.N. Biyushkin, T.I. Malinovski, L.D. Protsenko, T.N. Dneprova, Dokl. AN USSR 266 (1982) 1391.
- [6] E.A. Trush, V.M. Amirkhanov, V.A. Ochynnikov, J.S. Kozłowska, K.A. Lanikina, K.V. Domasevitch, Polyhedron 22 (2003) 1221.
- [7] K. Gholivand, F. Mojahed, M. Salehi, A. Madani, Anal. Sci. 22 (2006) x13.
- [8] M.L. Helm, S.A. Katz, T.W. Imioczyk, R.M. Hands, A.O. Norman, Inorg. Chem. 38 (1999) 3167.
- [9] S.E. Denmark, K.A. Swiss, S.R. Wilson, J. Am. Chem. Soc. 115 (1993) 3826.
- [10] K.V. Katti, A.A. Pinkerton, R.G. Cavell, Inorg. Chem. 30 (1991) 2631.
- [11] V.V. Skopenko, V.M. Amirkhanov, V.A. Ovchinnikov, A.V. Turov, Russ. J. Inorg. Chem. 41 (1996) 589.
- [12] V.A. Ovchinnikov, V.M. Amirkhanov, K.V. Domasevich, I. Siler, V.V. Skopenko, Zh. Neorg. Khim 46 (2001) 615.
- [13] K. Gholivand, Z. Shariatnia, M. Pourayoubi, Z. Anorg. Allg. Chem. 632 (2006) 160.
- [14] K. Gholivand, Z. Shariatnia, M. Pourayoubi, Z. Anorg. Allg. Chem. 631 (2005) 961.
- [15] E.A. Bundy, V.M. Amirkhanov, V.A. Ovchinnikov, V.A. Trush, K.V. Domasevitch, J. Sieler, V.V. Skopenko, Z. Naturforsch. 54 (1999) 1033.
- [16] K.E. Gubina, V.A. Ovchinnikov, J. Swiatek-Kozłowska, V.M. Amirkhanov, T.Y. Sliva, K.V. Domasevitch, Polyhedron 21 (2002) 963.
- [17] K. Gholivand, N. Oroujzadeh, F. Afshar, J. Organomet. Chem. 695 (2010) 1383.
- [18] K. Gholivand, N. Oroujzadeh, M. Rajabi, J. Iran. Chem. Soc. 9 (2012) 865.
- [19] P. Dorkov, I. Pantcheva, W. Sheldrick, H. Figge, R. Petrova, M. Mitewa, J. Inorg. Biochem. 102 (2008) 26.
- [20] S. Mandal, A. Rout, A. Ghosh, G. Pilet, D. Bandyopadhyay, Polyhedron 28 (2009) 3858.
- [21] L. Jin, F. Xiao, G. Cheng, Z. Ji, Inorg. Chem. Commun. 9 (2006) 758.
- [22] M. Li, C. Chen, D. Zhang, J. Niu, B. Ji, Eur. J. Med. Chem. 45 (2010) 3169.
- [23] D. Zhou, Q. Chen, Y. Qi, H. Fu, Z. Li, K. Zhao, J. Gao, Inorg. Chem. 50 (2011) 6929.
- [24] X. Chen, L. Tang, Y. Sun, P. Qiu, G. Liang, J. Inorg. Biochem. 104 (2010) 1141.
- [25] D.P. Singh, K. Kumar, C. Sharma, Eur. J. Med. Chem. 45 (2010) 1230.
- [26] G. Mohamed, M. Soliman, Spectrochim. Acta, Part A 76 (2010) 341.
- [27] (a) S.T. Castaman, S. Nakagaki, R.R. Ribeiro, K.J. Ciuffi, S.M. Drechsel, J. Mol. Catal. A: Chem. 300 (2009) 89; (b) J.R. Lindsay-Smith, B.C. Gilbert, A.M. Payeras, J. Murray, T.R. Lowdon, J. Oakes, R.P. Prats, P.H. Walton, J. Mol. Catal. A: Chem. 251 (2006) 114; (c) G.B. Shul'pin, G. Suss-Fink, L.S. Shul'pina, J. Mol. Catal. A: Chem. 170 (2001) 17.
- [28] K. Gholivand, M. Rajabi, F. Molaei, H.R. Mahzouni, S. Farshadian, J. Coord. Chem. 66 (2013) 4199.
- [29] Z. Otwinowsky, W. Minor, in: C.W. Carter Jr., R.M. Sweet (Eds.), Methods in Enzymology, vol. 276: Macromolecular Crystallography, Part A, Academic Press, New York, 1997, p. 307.
- [30] M.C. Burla, R. Caliandro, M. Camalli, B. Carrozzini, G.L. Cascarano, L. De Caro, C. Giacovazzo, G. Polidori, R. Spagna, J. Appl. Crystallogr. 38 (2005) 381.
- [31] G.M. Sheldrick, Acta Crystallogr., Sect. A64 (2008) 112.
- [32] A.L. Spek, Acta Crystallogr., Sect. D65 (2009) 148.
- [33] M.J. Frisch, G.W. Trucks, H.B. Schlegel, G.E. Scuseria, M.A. Robb, J.R. Cheeseman, V.G. Zakrzewski, J.A. Montgomery Jr., R.E. Stratmann, J.C. Burant, S. Dapprich,

- J.M. Millam, A.D. Daniels, K.N. Kudin, M.C. Strain, O. Farkas, J. Tomasi, V. Barone, M. Cossi, R. Cammi, B. Mennucci, C. Pomelli, C. Adamo, S. Clifford, J. Ochterski, G.A. Petersson, P.Y. Ayala, Q. Cui, K. Morokuma, D.K. Malick, A.D. Rabuck, K. Raghavachari, J.B. Foresman, J. Cioslowski, J.V. Ortiz, A.G. Baboul, B.B. Stefanov, G. Liu, A. Liashenko, P. Piskorz, I. Komaromi, R. Gomperts, R.L. Martin, D.J. Fox, T. Keith, M.A. Al-Laham, C.Y. Peng, A. Nanayakkara, C. Gonzalez, M. Challacombe, P.M.W. Gill, B. Johnson, W. Chen, M.W. Wong, J.L. Andres, C. Gonzalez, M. Head-Gordon, E.S. Replogle, J.A. Pople, *GAUSSIAN 03*, Revision B.03, Gaussian Inc., Wallingford, CT, 2004.
- [34] C. Lee, W. Yang, R.G. Parr, *Phys. Rev. B* 36 (1988) 785.
- [35] C.W. Bauschlicher Jr., *Chem. Phys. Lett.* 246 (1995) 40.
- [36] A.E. Reed, L.A. Curtiss, F. Weinhold, *Chem. Rev.* 88 (1988) 899.
- [37] F. Biegler-Konig, J. Schonbohm, D. Bayles, *J. Comput. Chem.* 22 (2001) 545.
- [38] A. Ataç, S. Yurdakul, S. Ide, *J. Mol. Struct.* 783 (2006) 79.
- [39] (a) S. Akyüz, A.B. Dempster, R.L. Morehouse, S. Suzuki, *J. Mol. Struct.* 17 (1973) 105;
(b) S. Suzuki, W.J. Orville-Thomas, *J. Mol. Struct.* 37 (1977) 321;
(c) M. Bakiler, I.V. Maslov, S. Akyüz, *J. Mol. Struct.* 476 (1999) 21.
- [40] O. Treu Filho, J.C. Pinheiro, E.B. da Costa, R.T. Kondo, R.A. de Souza, V.M. Nogueira, A.E. Mauro, *J. Mol. Struct. Theochem* 763 (2006) 175.
- [41] (a) K. Gholivand, Z. Shariatinia, M. Pourayoubi, *Polyhedron* 25 (2006) 711;
(b) K. Gholivand, Z. Shariatinia, *J. Organomet. Chem.* 691 (2006) 4215.
- [42] K. Gholivand, H.R. Mahzouni, M. Pourayoubi, S. Amiri, *Inorg. Chim. Acta* 363 (2010) 2318.
- [43] (a) C.E. Griffin, M. Gordon, *J. Org. Chem.* 3 (1965) 414;
(b) W.G. Bentrude, E.R. Witt, *J. Am. Chem. Soc.* 85 (1963) 2522;
(c) F. Kaplan, G. Singh, H. Zimmer, *J. Phys. Chem.* 67 (1963) 2509;
(d) K. Gholivand, S. Ghadimi, H. Naderimanes, A. Forouzanfar, *Magn. Reson. Chem.* 39 (2001) 684.
- [44] (a) W. Park, J.H. Cho, H.I. Lee, M. Park, M.S. Lah, D. Lim, *Polyhedron* 27 (2008) 2043;
(b) X. Zhang, K. Cheng, *J. Coord. Chem.* 65 (2012) 3019.
- [45] K.E. Gubina, O.A. Maslov, E.A. Trush, V.A. Trush, V.A. Ovchinnikov, S.V. Shishkina, V.M. Amirkhanov, *Polyhedron* 28 (2009) 2661.
- [46] (a) I. Szekeley, C. Silvestru, J.E. Drake, G. Balazs, S.I. Farcas, I. Haiduc, *Inorg. Chim. Acta* 299 (2000) 247;
(b) I. Szekeley, J.E. Drake, C. Silvestru, *Sulfur Silicon* 557 (1997) 124;
(c) A.M. Preda, A. Silvestru, S. Farcas, A. Bienko, J. Mrozinski, M. Andruh, *Polyhedron* 27 (2008) 2905;
(d) W. Shi, L. Zhang, M. Shafaei-Fallah, A. Rothenberger, *Z. Anorg. Allg. Chem.* 633 (2007) 440.
- [47] K. Gholivand, F. Molaei, M. Rajabi, M.D. Esrafil, M. Hosseini, *Polyhedron* 71 (2014) 8.
- [48] C. Boehme, G. Wipff, *Inorg. Chem.* 41 (2002) 727.
- [49] (a) K.E. Gubina, J.A. Shatrava, V.A. Ovchinnikov, V.M. Amirkhanov, *Polyhedron* 19 (2000) 2203;
(b) V.A. Trush, K.E. Gubina, V.M. Amirkhanov, J. Swiatek-Kozłowska, K.V. Domasevitch, *Polyhedron* 24 (2005) 1007;
(c) K. Gholivand, S. Farshadian, *Inorg. Chim. Acta* 368 (2011) 111;
(d) R.V. Yizhak, K.O. Znovjyak, V.A. Ovchinnikov, T.Y. Sliva, I.S. Konovalova, V.V. Medvediev, O.V. Shishkin, V.M. Amirkhanov, *Polyhedron* 62 (2013) 293.
- [50] (a) M.T. Ben Dhia, M.A.M.K. Sanhoury, L.C. Owono, M.R. Khaddar, *J. Mol. Struct.* 892 (2008) 103;
(b) K. Essalah, M.A. Sanhoury, M.T. Ben, *J. Mol. Struct. Theochem* 942 (2010) 110.
- [51] (a) R.F.W. Bader, *Atoms in Molecules: A Quantum Theory*, Oxford University Press, Oxford, UK, 1984;
(b) R.F.W. Bader, *Chem. Rev.* 91 (1991) 893.
- [52] D. Cremer, E. Kraka, *Angew. Chem., Int. Ed.* 23 (1984) 627.
- [53] E. Reed, L.A. Curtiss, F. Weinhold, *Chem. Rev.* 88 (1988) 899.
- [54] (a) U. Sundermeier, C. Dobler, M. Beller, in: J.E. Backvall (Ed.), *Modern Oxidation Methods*, Wiley-VCH, Weinheim, 2004;
(b) B.S. Lane, K. Burgess, *Chem. Rev.* 103 (2003) 2457;
(c) K.A. Joergensen, *Chem. Rev.* 89 (1989) 431;
(d) L. Que, W.B. Tolman, *J. Nat.* 455 (2008) 333.
- [55] D.P. Kessissoglou, *Coord. Chem. Rev.* 837 (1999) 185.
- [56] K.P. Ho, W.L. Wong, K.M. Lam, C.P. Lai, T.H. Chan, K.Y. Wong, *Chem. Eur. J.* 14 (2008) 7988.
- [57] O. Cusó, I. Garcia-Bosch, D. Font, X. Ribas, J. Lloret-Fillol, M. Costas, *Org. Lett.* 15 (2013) 6158.
- [58] (a) P. Battioni, J.P. Renaud, J.F. Bartoli, M. Reina-Artiles, M. Fort, D. Mansuy, *J. Am. Chem. Soc.* 110 (1988) 8462;
(b) P. Tagliatesta, D. Giovannetti, A. Leoni, M.G.P.M.S. Neves, J.A.S. Cavaleiro, *J. Mol. Catal. A* 252 (2006) 96.